J|A|C|S ARTICLES

Published on Web 08/18/2010

Double Protonation of 1,5-Bis(triarylaminoethynyl)anthraquinone To Form a Paramagnetic Pentacyclic Dipyrylium Salt

Koya Prabhakara Rao, Tetsuro Kusamoto, Fumiyuki Toshimitsu, Kiyotaka Inayoshi, Shoko Kume, Ryota Sakamoto, and Hiroshi Nishihara*

Department of Chemistry, School of Science, The University of Tokyo, 7-3-1 Hongo, Bunkyo-ku, Tokyo 113-0033, Japan

Received June 16, 2010; E-mail: nisihara@chem.s.u-tokyo.ac.jp

Abstract: Protonation-induced intramolecular cyclization reactions of new donor (D)−acceptor (A) and D−A−D conjugated molecules 1-triarylaminoethynylanthraquinone (**1-AmAq**) and 1,5-bis(triarylaminoethynyl)anthraquinone (**1,5-Am$_2$Aq**), respectively, were achieved. The former undergoes monoprotonation with bis(trifluoromethanesulfone)imide acid (TFSIH) to give pyrylium salt **[1-AmPyl]TFSI**, whereas the latter undergoes a novel double proton cyclization reaction to yield 1,5-bis(triarylamino)dipyrylium salt **[1,5-Am$_2$Pyl$_2$](TFSI)$_2$** with a new pentacyclic backbone. This divalent cationic salt can be reduced to give the neutral species 2,8-bis(triarylamino)benzo[*de*]isochromeno[1,8-*gh*]chromene (**[1,5-Am$_2$Pyl$_2$]^0**), which maintains the planar pentacyclic backbone. The obtained condensed-ring compounds show unique optical, electrochemical, and magnetic properties due to the extremely narrow HOMO−LUMO gap. In particular, the dication **[1,5-Am$_2$Pyl$_2$]$^{2+}$** shows paramagnetic behavior with *two spins* centered on two triarylamine moieties through valence tautomerization with the pentacyclic backbone.

Introduction

Donor (D)−acceptor (A) compounds are exciting materials,[1] particularly for controlling electronic communication by external stimuli,[2−4] such as protons, photons, and electrons. Because the electronic structure of a molecule directly influences its physical properties,[5−7] the electronic properties can be employed to achieve switching behavior in molecular devices.[8,9]

We have previously described a new class of D−A molecules comprising a 1:1 donor/acceptor formula, **1-RAq**,[10−12] in which R (= ferrrocenyl (Fc), phenyl, *m*-tolyl, or *p*-tolyl) and Aq (anthraquinone) undergo intramolecular cyclization to give pyrylium cations **[1-RPyl]**$^+$. This phenomenon can be used to lower the energy of the lowest unoccupied molecular orbital

(1) (a) Joachim, C.; Gimzewski, J. K.; Aviram, A. *Nature*. **2000**, *408*, 541–548. (b) Seminario, J. M. *Nat. Mater.* **2005**, *4*, 111–113. (c) Ehli, C.; Oelsner, C.; Guldi, D. M.; Mateo-Alonso, A.; Prato, M.; Schmidt, C.; Backes, C.; Hauke, F.; Hirsch, A. *Nat. Chem.* **2009**, *1*, 243–249.

(2) (a) Sato, O.; Tao, J.; Zhang, Y.-Z. *Angew. Chem., Int. Ed.* **2007**, *46*, 2152–2187. (b) Mativetsky, J. M.; Pace, G.; Elbing, M.; Rampi, M. A.; Mayor, M.; Samorì, P. *J. Am. Chem. Soc.* **2008**, *130*, 9192–9193. (c) Klajn, R.; Fang, L.; Coskun, A.; Olson, M. A.; Wesson, P. J.; Stoddart, J. F.; Grzybowski, B. A. *J. Am. Chem. Soc.* **2009**, *131*, 4233–4235. (d) Champin, B.; Mobian, P.; Sauvage, J.-P. *Chem. Soc. Rev.* **2007**, *36*, 358–366.

(3) (a) Kume, S.; Murata, M.; Ozeki, T.; Nishihara, H. *J. Am. Chem. Soc.* **2005**, *127*, 490–491. (b) Sakamoto, R.; Murata, M.; Kume, S.; Sampei, S.; Sugimoto, M.; Nishihara, H. *Chem. Commun.* **2005**, 1215–1217. (c) Muratsugu, S.; Kume, S.; Nishihara, H. *J. Am. Chem. Soc.* **2008**, *130*, 7204–7205.

(4) (a) Sakamoto, A.; Hirooka, A.; Namiki, K.; Kurihara, M.; Murata, M.; Sugimoto, M.; Nishihara, H. *Inorg. Chem.* **2005**, *44*, 7547–7558. (b) Colbran, S. B.; Lee, S. T.; Lonnon, D. G.; Maharaj, F. J. D.; McDonagh, A. M.; Walker, K. A.; Young, R. D. *Organometallics* **2006**, *25*, 2216–2224. (c) Kondo, M.; Murata, M.; Nishihara, H.; Nishibori, E.; Aoyagi, S.; Yoshida, M.; Kinoshita, Y.; Sakata, M. *Angew. Chem., Int. Ed.* **2006**, *45*, 5461–5464.

(5) (a) Ratera, I.; Molina, D. R.; Renz, F.; Ensling, J.; Wurst, K.; Rovira, C.; Gütlich, P.; Veciana, J. *J. Am. Chem. Soc.* **2003**, *125*, 1463–1464. (b) Jiao, J.; Long, G. J.; Grandjean, F.; Beatty, A. M.; Fehlner, T. P. *J. Am. Chem. Soc.* **2003**, *125*, 7522–7523. (c) Nishihara, H. *Adv. Inorg. Chem.* **2002**, *53*, 41–86. (d) Hillard, E.; Vessieres, A.; Thouin, L.; Jaouen, G.; Amatore, C. *Angew. Chem., Int. Ed.* **2006**, *45*, 285–290. (e) Albinati, A.; Fabrizi de Biani, F.; Leoni, P.; Marchetti, L.; Pasquali, M.; Rizzato, S.; Zanello, P. *Angew. Chem., Int. Ed.* **2005**, *44*, 5701–5705.

(6) (a) Green, J. E.; Choi, J. W.; Boukai, A.; Bunimovich, Y.; Halperin, E. J.; DeIonno, E.; Luo, Y.; Sheriff, B. A.; Xu, K.; Shin, Y. S.; Tseng, H.-R.; Stoddart, J. F.; Heath, J. R. *Nature* **2007**, *445*, 414–417. (b) Irie, M. *Chem. Rev.* **2000**, *100*, 1685–1716. (c) Sakamoto, R.; Kume, S.; Nishihara, H. *Chem.—Eur. J.* **2008**, *14*, 6978–6986. (d) Nagashima, S.; Murata, M.; Nishihara, H. *Angew. Chem., Int. Ed.* **2006**, *45*, 4298–4301.

(7) (a) Gabelica, V.; Kresge, A. J. *J. Am. Chem. Soc.* **1996**, *118*, 3838–3841. (b) Rowan, S. J.; Cantrill, S. J.; Cousins, G. R. L.; Sanders, J. K. M.; Stoddart, J. F. *Angew. Chem., Int. Ed.* **2002**, *41*, 898–952. (c) Arai, R.; Uemura, S.; Irie, M.; Matsuda, K. *J. Am. Chem. Soc.* **2008**, *130*, 9371–9379. (d) Duriska, M. B.; Neville, S. M.; Moubaraki, B.; Cashion, J. D.; Halder, G. J.; Chapman, K. W.; Balde, C.; Létard, J.-F.; Murray, K. S.; Kepert, C. J.; Batten, S. R. *Angew. Chem., Int. Ed.* **2009**, *48*, 2549–2552.

(8) (a) Dediu, V. A.; Hueso, L. E.; Bergenti, I.; Taliani, C. *Nat. Mater.* **2009**, *8*, 707–716. (b) Gundlach, D. J.; et al. *Nat. Mater.* **2008**, *7*, 216–221. (c) Huang, Y. S.; Westenhoff, S.; Avilov, I.; Sreearunothai, P.; Hodgkiss, J. M.; Deleener, C.; Friend, R. H.; Beljonne, D. *Nat. Mater.* **2008**, *7*, 483–489. (d) Tian, H.; Yang, X.; Pan, J.; Chen, R.; Liu, M.; Zhang, Q.; Hagfeldt, A.; Sun, L. *Adv. Funct. Mater.* **2008**, *18*, 3461–3468.

(9) (a) Ross, R. B.; Cardona, C. M.; Guldi, D. M.; Sankaranarayanan, S. G.; Reese, M. O.; Kopidakis, N.; Peet, J.; Walker, B.; Bazan, G. C.; Van Keuren, E.; Holloway, B. C.; Drees, M. *Nat. Mater.* **2009**, *8*, 208–212. (b) Qian, G.; Zhong, Z.; Luo, M.; Yu, D.; Zhang, Z.; Wang, Z. Y.; Ma, D. *Adv. Mater.* **2009**, *21*, 111–116. (c) Park, S.; Seo, J.; Kim, S. H.; Park, S. Y. *Adv. Funct. Mater* **2008**, *18*, 726–731.

10.1021/ja105250f

Table 1. Crystal Data and Structure Refinement Parameters for **1-AmAq**, **1,5-Am$_2$Aq**, and **[1,5-Am$_2$Pyl$_2$]^0**

	1-AmAq	1,5-Am$_2$Aq	[1,5-Am$_2$Pyl$_2$]^0
empirical formula	$C_{36}H_{25}NO_4$	$C_{58}H_{42}N_2O_6$	$C_{59}H_{46}Cl_2N_2O_6$
crystal system	triclinic	monoclinic	monoclinic
space group	$P\bar{1}$	$P2_1/c$	$P2_1/c$
crystal size (mm)	0.5 × 0.2 × 0.2	0.3 × 0.2 × 0.1	0.2 × 0.2 × 0.1
a (Å)	9.752(2)	15.703(8)	19.183(4)
b (Å)	11.925(3)	10.301(4)	12.104(2)
c (Å)	12.577(3)	15.738(8)	21.435(4)
α (°)	102.896(2)	90.0	90.0
β (°)	107.463(4)	119.718(6)	111.302(2)
γ (°)	95.645(2)	90.0	90.0
V (Å^3)	1338.4(5)	2210.9(18)	4637.1(15)
Z	2	2	4
formula mass	535.57	862.94	949.88
ρ_{calc} (g cm^{-3})	1.329	1.296	1.361
λ (Mo Kα) Å	0.71073	0.71073	0.71073
μ (mm^{-1})	0.087	0.084	0.198
θ range (°)	3.09−27.47	3.25−27.43	3.16−27.50
total data collected	10 651	16 931	35 773
unique data	5860	5009	10 600
observed data ($I > 2\sigma(I)$)	4329	3066	8027
R indexes [$I > 2\sigma(I)$]	$R_1 = 0.0475$, $wR_2 = 0.1386$	$R_1 = 0.0823$, $wR_2 = 0.1698$	$R_1 = 0.0912$, $wR_2 = 0.2545$
goodness of fit	1.032	1.101	1.070

(LUMO), which allows intramolecular electron transfer, thereby generating valence tautomers,[13,14] especially in compounds with a strong donor, such as **1-FcAq**.[11] In addition, **1-RAq** undergoes alcohol- and acid-induced reversible switching, as observed in the near-infrared (NIR) absorption band for R = Fc and in the luminescence emission band for R = Ph, *m*-tolyl, or *p*-tolyl.[15] We also reported the double protonation of 1,5-bis(ferrocenyl)-anthraquinone (**1,5-Fc$_2$Aq**)[16] to give a paramagnetic molecule with unique optical properties, but its chemical structure must be reinvestigated in light of the discovery of the cyclization reaction of **1-FcAq**[11] at this stage.

In the present study, we report the synthesis and characterization of new D−A and D−A−D molecules containing triarylamine as the donor: 1-triarylaminoethynylanthraquinone (**1-AmAq**) and 1,5-bis(triarylaminoethynyl)anthraquinone (**1,5-Am$_2$Aq**), respectively. The former undergoes monoprotonation to give a pyrylium salt, **[1-AmPyl]TFSI**, similar to **1-FcAq**.[11] The latter undergoes a novel double proton cyclization reaction to yield a 1,5-bis(triarylamino)dipyrylium salt, **[1,5-Am$_2$Pyl$_2$](TFSI)$_2$**, with a new type of pentacyclic backbone. This divalent cation can be reduced to give the neutral species 2,8-bis(triarylamino)benzo[*de*]isochromeno[1,8-*gh*]chromene (**[1,5-Am$_2$Pyl$_2$]^0**) that preserves the planar pentacyclic backbone. The obtained condensed-ring compounds with narrow HOMO−LUMO gap show unique optical, electrochemical, and magnetic properties. In particular, the dication **[1,5-Am$_2$Pyl$_2$]$^{2+}$** shows not diamagnetic but paramagnetic behavior, with two spins centered on two triarylamine moieties. The synthesis, characterization, X-ray structures, and chemical and physical properties of the triarylaminoethynylanthraquinones and their protonated products are described in this paper.

Results and Discussion

Synthesis and Characterization of 1-AmAq and 1,5-Am$_2$Aq. **1-AmAq** and **1,5-Am$_2$Aq** were synthesized by the Sonogashira cross-coupling of 1-ethynyltriarylamine with 1-bromoanthraquinone and 1,5-dibromoanthraquinone, respectively. Single crystals of each were obtained by recrystallization from dichloromethane (DCM)/hexane at 293 K, and their molecular structures were determined by single-crystal X-ray diffraction analysis (Table 1). ORTEP drawings of both compounds are shown in Figure 1, in which D and A moieties are on the same plane.

Formation and Properties of [1-AmPyl]TFSI. The cyclocondensation reaction of **1-AmAq** was performed using bis(trifluoromethanesulfone)imide acid (TFSIH) as a proton source (Scheme 1). The UV−vis−NIR spectral changes upon addition of TFSIH in DCM displayed an isosbestic point similar to that of **1-FcAq**, and absorption peaks appeared at 474 and 846 nm (Supporting Information, Figure S1), which were assignable to HOMO (140) (triarylamine π)−LUMO+1 (142) (pyrylium π^*) and HOMO (140)−LUMO (141) (pyrylium π^*) transitions, respectively, based on time-dependent density functional theory (TD-DFT) calculations. The latter is a typical intervalence charge-transfer (IVCT) band for D−A conjugated molecules. The spectral changes were accompanied by a solution color change from yellow to deep red. The protonated product was isolated and characterized by ^{1}H NMR and IR spectroscopy and

(10) Murata, M.; Fujita, T.; Yamada, M.; Kurihara, M.; Nishihara, H. *Chem. Lett.* **2000**, 1328–1329.
(11) Kondo, M.; Uchikawa, M.; Zhang, W.-W.; Namiki, K.; Kume, S.; Murata, M.; Kobayashi, Y.; Nishihara, H. *Angew. Chem., Int. Ed.* **2007**, *46*, 6271–6274.
(12) Kondo, M.; Uchikawa, M.; Namiki, K.; Zhang, W.; Kume, S.; Nishibori, E.; Suwa, H.; Aoyagi, S.; Sakata, M.; Murata, M.; Kobayashi, Y.; Nishihara, H. *J. Am. Chem. Soc.* **2009**, *131*, 12112–12124.
(13) (a) Tao, J.; Maruyama, H.; Sato, O. *J. Am. Chem. Soc.* **2006**, *128*, 1790–1791. (b) Diallo, A. K.; Daran, J.-C.; Varret, F.; Ruiz, J.; Astruc, D. *Angew. Chem., Int. Ed.* **2009**, *48*, 3141–3145. (c) Mochida, T.; Takazawa, K.; Matsui, H.; Takahashi, M.; Takeda, M.; Sato, M.; Nishio, Y.; Kajita, K.; Mori, H. *Inorg. Chem.* **2005**, *44*, 8628–8641. (d) Salamon, S. B.; Brewer, S. H.; Depperman, E. C.; Franzen, S.; Kampf, J. W.; Kirk, M. L.; Kumar, R. K.; Lappi, S.; Peariso, K.; Preuss, K. E.; Shultz, D. A. *Inorg. Chem.* **2006**, *45*, 4461–4467. (e) Hearns, N. G. R.; Korèok, J. L.; Paquette, M. M.; Preuss, K. E. *Inorg. Chem.* **2006**, *45*, 8817–8819.
(14) (a) Rotthaus, O.; Thomas, F.; Jarjayes, O.; Philouze, C.; Saint-Aman, E.; Pierre, J.-L. *Chem.−Eur. J.* **2006**, *12*, 6953–6962. (b) Naumov, P.; Belik, A. A. *Inorg. Chem. Commun.* **2008**, *11*, 465–469. (c) Kiriya, D.; Chang, H.-C.; Nakamura, K.; Tanaka, D.; Yoneda, K.; Kitagawa, S. *Chem. Mater.* **2009**, *21*, 1980–1988.
(15) Kondo, M.; Uchikawa, M.; Kume, S.; Nishihara, H. *Chem. Commun.* **2009**, *15*, 1993–1995.
(16) Murata, M.; Yamada, M.; Fujita, T.; Kojima, K.; Kurihara, M.; Kubo, K.; Kobayashi, Y.; Nishihara, H. *J. Am. Chem. Soc.* **2001**, *123*, 12903–12904.

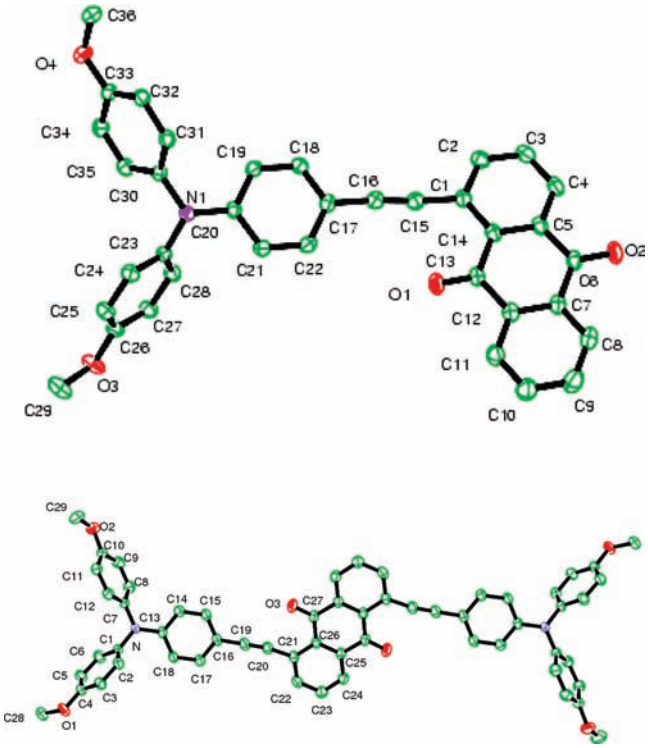

Figure 1. ORTEP diagrams (50% probability, hydrogen atoms are omitted for clarity) of **1-AmAq** (top) and **1,5-Am$_2$Aq** (bottom).

by elemental analysis to determine a tetracyclic pyrylium cation structure, **[1-AmPyl]**$^+$, similar to that of **[1-FcPyl]**$^+$ [11] (Supporting Information, Figure S2).

The cyclic voltammogram of **[1-AmPyl]**$^+$ in 0.1 M Bu_4NClO_4−CH_2Cl_2 displayed one reversible oxidation wave at +0.49 V vs ferrocenium/ferrocene (Fc^+/Fc) and two reversible reduction waves at −0.11 and −1.06 V (Supporting Information, Figure S3). In contrast, the cyclic voltammogram of **1-AmAq** showed an oxidation wave at +0.25 V and reduction waves at −1.42 and −1.85 V, indicating significant narrowing of the difference between the oxidation potential and the first reduction potential from 1.67 to 0.60 V upon protonation (Table 2, Figure 2, and Figure S3).

Similarities between **[1-AmPyl]**$^+$ and **[1-FcPyl]**$^+$ were also observed in terms of their chemical reactivities.[15] **[1-AmPyl]**$^+$ reacted readily with sodium methoxide in methanol to afford a yellow neutral acetal compound, **1-AmPyl-OMe** (Scheme 1), which was characterized using NMR techniques: ^{1}H NMR, ^{13}C NMR, COSY, HMQC, and HMBC methods (Supporting Information, Figures S4 and S5). Upon formation of the acetal derivative, the characteristic UV−vis−NIR absorption bands at 490 and 840 nm disappeared (Supporting Information, Figure S6). **1-AmPyl-OMe** reversibly returned to **[1-AmPyl]**$^+$ upon treatment with TFSIH (Figure S6).

Protonation of 1,5-Am$_2$Aq and Properties of the Products. The protonation-induced cyclization reaction of **1,5-Am$_2$Aq** with the acid TFSIH in DCM was monitored by UV−vis−NIR absorption spectroscopy. As shown in Figure 3, the spectrum changed in two steps, indicating that two protonation reactions occurred sequentially. First, the band at 395 nm corresponding to the anthraquinone moiety decreased and the band at 495 nm, characteristic of the pyrylium ring, grew along with several new bands at 550−900 nm and a broad IVCT band at 1100−2200 nm with λ_{max} = 1400 nm. Subsequently, the spectrum did not change, except that the intensity of the broad IVCT band at 1100−2200 nm increased further while retaining the same λ_{max}. The small bands at 690 and 760 nm were assigned to the formation a π radical cation.[17] The **1,5-Am$_2$Aq** solution turned from deep red to greenish yellow after the addition of 2 equiv of TFSIH.

The cyclization products of the mono- and diprotonated salts **[1,5-Am$_2$Pyl]TFSI** and **[1,5-Am$_2$Pyl$_2$](TFSI)$_2$** were synthesized under an argon atmosphere by the addition of 1 and 4 equiv of TFSIH in DCM, affording yields of 89% and 92%, respectively. The formation of a pentacyclic compound was suggested by the single-crystal X-ray crystallography of **[1,5-Am$_2$Pyl$_2$]-(TFSI)$_2$**, although the analysis was not sufficient because of the instability of single crystals in ambient conditions (see Supporting Information, including Figure S7, for details). The FTIR spectra shown in Figure S8 (Supporting Information) showed that the C≡C stretching vibration of the acetylene moiety at 2208 cm^{-1} and the C═O vibration of the quinone moiety at 1670 cm^{-1} observed in the spectrum of **1,5-Am$_2$Aq** disappeared completely in the protonated product **[1,5-Am$_2$Pyl$_2$](TFSI)$_2$**. These spectral changes indicate that both ethylene moieties reacted with the proton, and the cyclocondensation reaction proceeded. The monoprotonated compound **[1,5-Am$_2$Pyl]TFSI** did not display a C≡C stretching vibration from the acetylene moiety due to the expansion of π-conjugation, in agreement with the UV−vis−NIR results. The C═O vibration of the quinone moiety was observed at 1670 cm^{-1}, as expected, with a decrease in intensity. The vibrations of the $TFSI^-$ ion were observed at 1351, 1195, 739, and 569 cm^{-1}, and the C═O vibrations of the pyrylium moieties were observed at 1594, 1525, and 1487 cm^{-1} for both **[1,5-Am$_2$Pyl]TFSI** and **[1,5-Am$_2$Pyl$_2$](TFSI)$_2$**. These results indicate that **[1,5-Am$_2$Pyl$_2$]-(TFSI)$_2$** has a pentacyclic structure constructed by the two-step cyclocondensation reaction of the acetylene moiety and the carbonyl group of the quinone moiety.

TD-DFT calculations were performed for the monoprotonated product **[1,5-Am$_2$Pyl]**$^+$ and the diprotonated product **[1,5-Am$_2$Pyl$_2$]**$^{2+}$, and the energies associated with excitation to the lowest excited states were estimated (see Supporting Information, Tables S1 and S2). The experimental excitation energies to the lowest excited state matched those calculated for the monocation **[1,5-Am$_2$Pyl]**$^+$. In contrast, the experimental and calculated excitation energies to the lowest excited state for the dication **[1,5-Am$_2$Pyl$_2$]**$^{2+}$ showed some variations, especially for the IVCT band, which may have been due to the existence of several valence tautomeric forms (Scheme 2). The calculations indicated that the absorption peaks at 495 and 760 nm (Figures 3 and 4) could be assigned to HOMO (226) (triarylamine)−LUMO+2 (229) (pyrylium) transitions. The IVCT bands for both **[1,5-Am$_2$Pyl]**$^+$ and **[1,5-Am$_2$Pyl$_2$]**$^{2+}$ were ascribed to HOMO (226) (triarylamine)−LUMO (227) (pyrylium) transitions. The IVCT band of **[1,5-Am$_2$Pyl$_2$]**$^{2+}$ was shifted to longer wavelengths relative to **[1-AmPyl]**$^+$ and **[1-FcPyl]**$^+$ [10,11] because its pentacyclic structure possesses a more extended π-conjugated system compared with the tetracyclic compounds. The lowering of the LUMO level in **[1,5-Am$_2$Pyl$_2$]**$^{2+}$ relative to other reported protonated compounds[10−12] was expected to produce more effective intramolecular charge transfer.

(17) (a) Hirao, Y.; Urabe, M.; Ito, A.; Tanaka, K. *Angew. Chem., Int. Ed.* **2007**, *46*, 3300–3303. (b) Sandberg, M. O.; Nagao, O.; Wu, Z.; Matsushita, M. M.; Sugawara, T. *Chem. Commun.* **2008**, 3738–3740.

Scheme 1. Cyclocondensation Reaction of **1-AmAq**

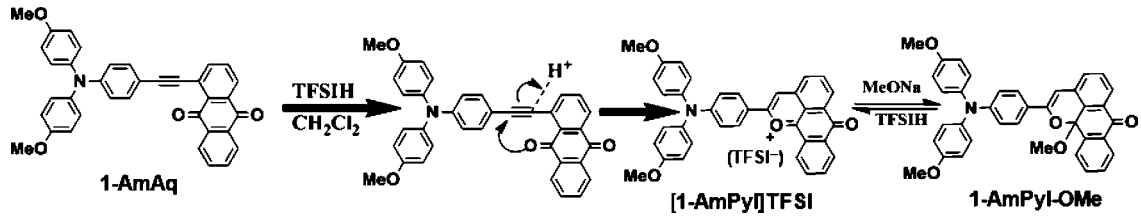

Table 2. Electrochemical Data of **1-AmAq**, **1,5-Am$_2$Aq**, **[1-AmPyl]$^+$**, **[1,5-Am$_2$Pyl]$^+$**, **[1,5-Am$_2$Pyl$_2$]$^{2+}$**, and **[1,5-Am$_2$Pyl$_2$]^0**

	oxidation (V vs Fc^+/Fc)		reduction (V vs Fc^+/Fc)	
compound	$E^{0\prime}$(ox1)	$E^{0\prime}$(ox2)	$E^{0\prime}$(red1)	$E^{0\prime}$(red2)
1-AmAq	0.25		−1.42	−1.85
[1-AmPyl]$^+$	0.49		−0.11	−1.06
1,5-Am$_2$Aq	0.30		−1.38	−1.82
[1,5-Am$_2$Pyl]$^+$	0.26	0.44	−0.14	−0.68
[1,5-Am$_2$Pyl$_2$]$^{2+}$	0.25	0.50	−0.06	−0.16

Cyclic voltammetry of **1,5-Am$_2$Aq**, **[1,5-Am$_2$Pyl]$^+$**, and **[1,5-Am$_2$Pyl$_2$]$^{2+}$** in 0.1 M Bu_4NClO_4−CH_2Cl_2 revealed two reversible one-electron reduction steps ascribed to the anthraquinone (Aq) and its protonated moieties (Pyl^+ and Pyl_2^{2+}) (Supporting Information, Figure S9). The reduction potentials were largely shifted to more positive values according to the sequential protonation steps (the shift in $E^{0\prime}$ for the first reduction between **[1,5-Am$_2$Pyl]$^+$** and **1,5-Am$_2$Aq** was 1.24 V, and that between **[1,5-Am$_2$Pyl$_2$]$^{2+}$** and **[1,5-Am$_2$Pyl]$^+$** was 0.08 V, Table 2), indicating a lowering of the LUMO, as expected. The nonprotonated form of **1,5-Am$_2$Aq** exhibited one reversible oxidation wave at $E^{0\prime}$ = 0.30 V vs Fc^+/Fc, and both protonated forms, **[1,5-Am$_2$Pyl]$^+$** and **[1,5-Am$_2$Pyl$_2$]$^{2+}$**, exhibited two oxidation waves at $E^{0\prime}$ = 0.26, 0.44 V and 0.25, 0.50 V, respectively. In agreement with the UV−vis−NIR absorption measurements, the HOMO−LUMO gap estimated from the difference between the first oxidation potential and the first reduction potential, $\Delta E^{0\prime}$, decreased with increasing π-conjugation (Figure 2). The $\Delta E^{0\prime}$ values for **[1,5-Am$_2$Pyl]$^+$** and **[1,5-Am$_2$Pyl$_2$]$^{2+}$** were 0.40 and 0.31 V, which were lowered by 1.28 and 1.39 V, respectively, after cyclization.

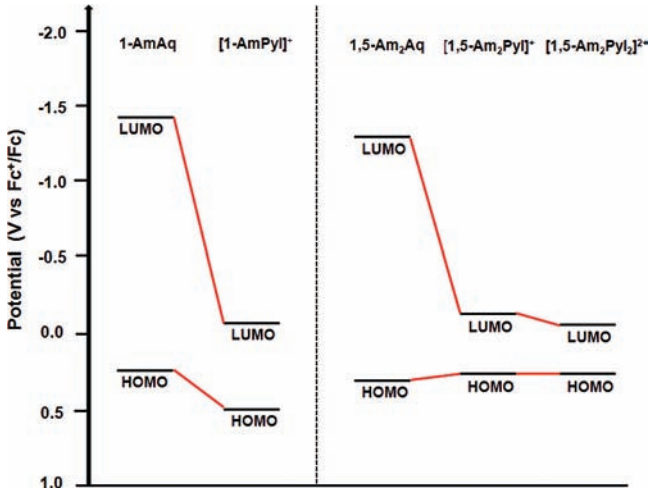

Figure 2. Schematic potential diagrams for **1-AmAq**, **1,5-Am$_2$Aq**, **[1-AmPyl]$^+$**, **[1,5-Am$_2$Pyl]$^+$**, **[1,5-Am$_2$Pyl$_2$]$^{2+}$**, and **[1,5-Am$_2$Pyl$_2$]^0** estimated from the redox potentials measured by cyclic voltammetry.

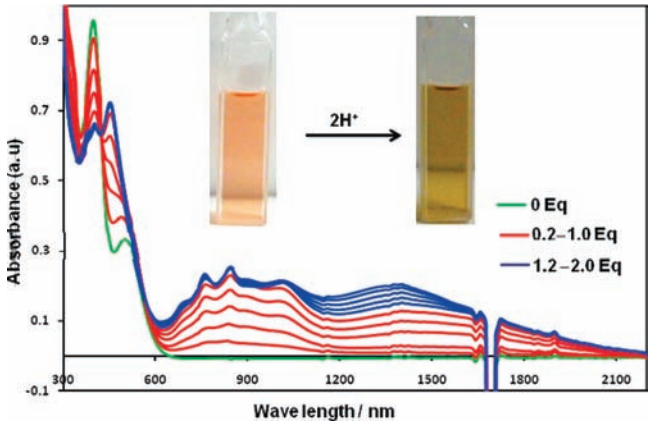

Figure 3. UV−vis−NIR absorption spectra of **1,5-Am$_2$Aq** in dichloromethane after each addition of TFSIH (bottom).

The protonated products **[1,5-Am$_2$Pyl]TFSI** and **[1,5-Am$_2$Pyl$_2$](TFSI)$_2$** were found to be NMR-silent (see Supporting Information, Figure S10), suggesting that they were paramagnetic. The DCM solutions of **[1,5-Am$_2$Pyl]TFSI** and **[1,5-Am$_2$Pyl$_2$](TFSI)$_2$** showed similar EPR spectra with different spin densities of 0.4 and 0.6 per molecule, respectively, based on the reference, 4-hydroxyl-2,2,6,6-tetramethylpiperidin-1-oxyl free radical. Because [**1-AmPyl]TFSI**, a compound related to **[1,5-Am$_2$Pyl]TFSI**, was diamagnetic, an additional D (= triarylamine) moiety was found to affect the formation of spins. It should be noted that the appearance of peaks at 690 and 760 nm was assignable to π-radicals[17] in the UV−vis−NIR spectrum of **[1,5-Am$_2$Pyl]TFSI**, but not in that of **[1-AmPyl]TFSI**, as noted above (compare Figures 3 and S1), supporting the difference in spin state between the two monocationic compounds.

The EPR spectrum of **[1,5-Am$_2$Pyl$_2$](TFSI)$_2$** at 100 K (Figure 5) showed a strong, broad signal at g = 2.003, which is a typical indication of π radical formation. At room temperature, the spectrum included 27 line spectra, which were assigned to hyperfine interactions resulting from the central N atoms and hydrogen atoms on the phenyl rings in the two triarylamine moieties.[17] This assignment was supported by simulated EPR spectra (Figure S9) with input consisting of the following experimental conditions: hyperfine coupling constants from the experimental data, the number of N atoms (two equivalent nitrogen atoms with a coupling constant of 0.235 mT), and the number of H atoms (12 equivalent hydrogen atoms with a coupling constant of 0.071 mT) (see scheme in Supporting Information, Figure S11). The simulated EPR spectra reasonably matched the experimental spectra. These results indicated that the spin density was distributed across two triarylamine moieties as a result of the (double) electron transfer from the electron-donating triarylamine moieties to the highly electron-accepting pentacyclic skeleton. The spin density value (0.6) per molecule uniformly distributed on two nitrogen atoms suggests that the paramagnetic tautomer was 30%, in equilibrium with the diamagnetic tautomer as shown in Scheme 2. The static

Scheme 2. Cyclocondensation Reaction of **1,5-Am$_2$Aq**

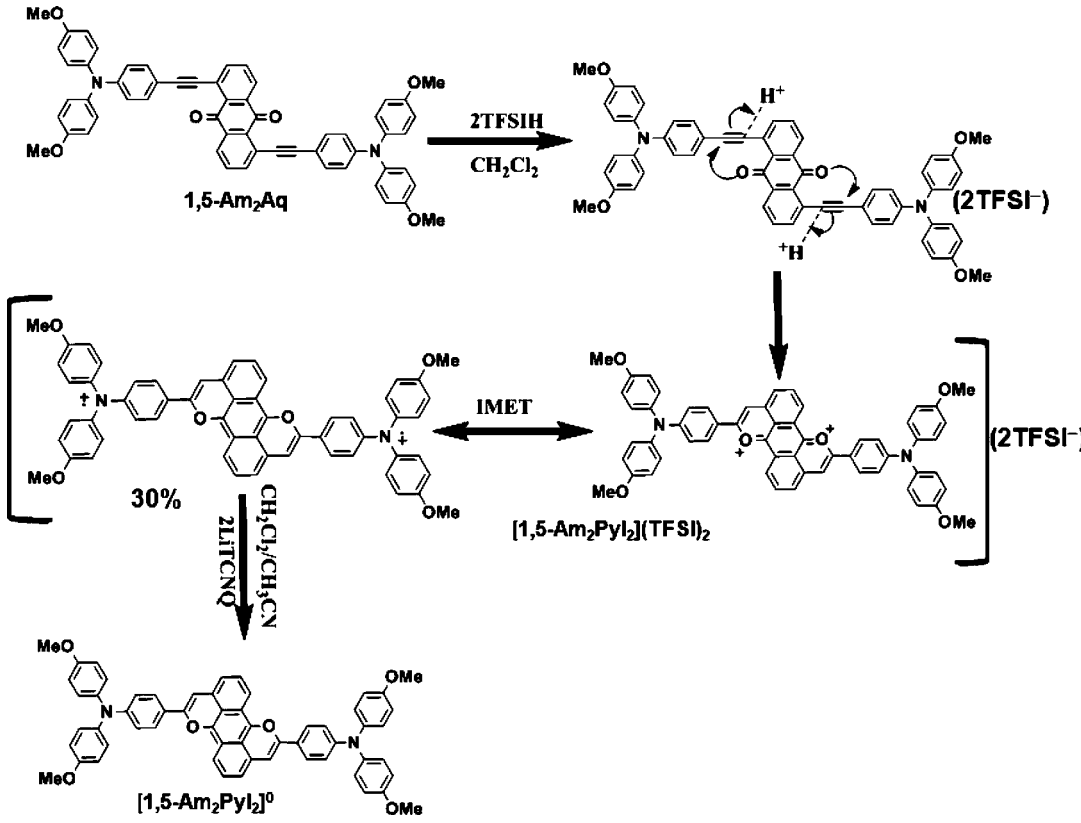

magnetic susceptibility measurements obtained using a SQUID magnetometer also demonstrated the paramagnetic nature of **[1,5-Am$_2$Pyl$_2$](TFSI)$_2$** with similar spin density (Supporting Information, Figure S12).

Preparation of the Neutral Form [1,5-Am$_2$Pyl$_2$]^0 by Reduction of [1,5-Am$_2$Pyl$_2$](TFSI)$_2$. The spectral results described above confirmed that lowering the LUMO allowed intramolecular electron transfer. Because the dicationic salt **[1,5-Am$_2$Pyl$_2$](TFSI)$_2$** was NMR-silent, had poor crystallinity (as noted above; see Supporting Information, including Figure S7), and underwent reversible two-step, one-electron reduction, we attempted to synthesize the neutral compound by chemical reduction to identify the exact structure of the protonated product.

The neutral compound **[1,5-Am$_2$Pyl$_2$]^0** was prepared by treatment of **[1,5-Am$_2$Pyl$_2$](TFSI)$_2$** with lithium tetracyano-

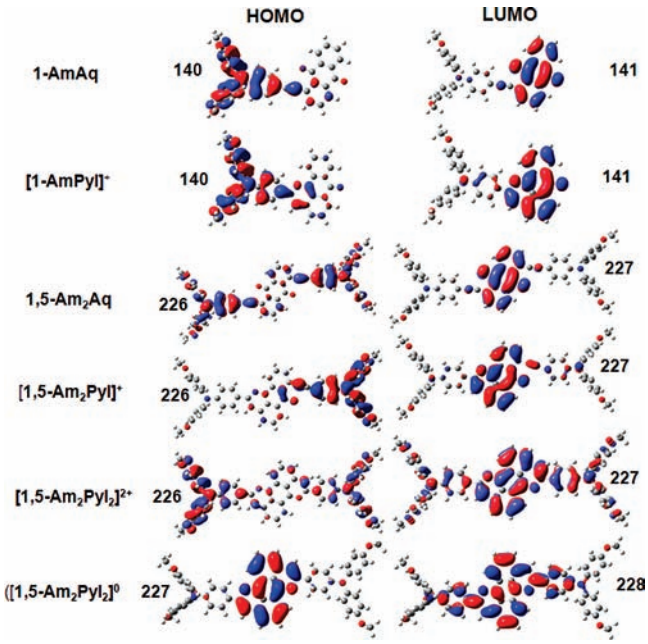

Figure 4. HOMO and LUMO energies calculated by the DFT method for **1-AmAq**, **1,5-Am$_2$Aq**, **[1-AmPyl]$^+$**, **[1,5-Am$_2$Pyl]$^+$**, **[1,5-Am$_2$Pyl$_2$]$^{2+}$**, and **[1,5-Am$_2$Pyl$_2$]^0**.

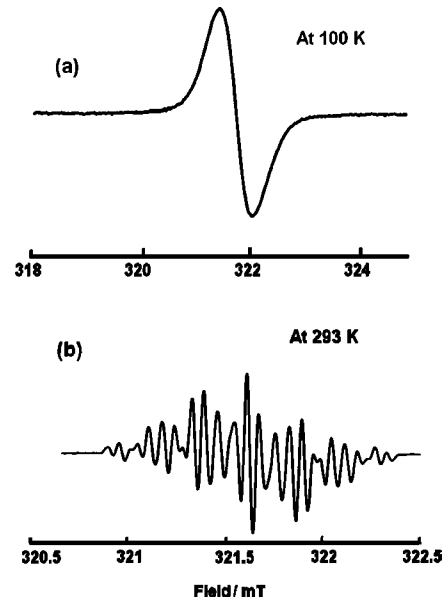

Figure 5. EPR spectra of **[1,5-Am$_2$Pyl$_2$](TFSI)$_2$** in CH_2Cl_2 solutions at (a) 100 K and (b) room temperature.

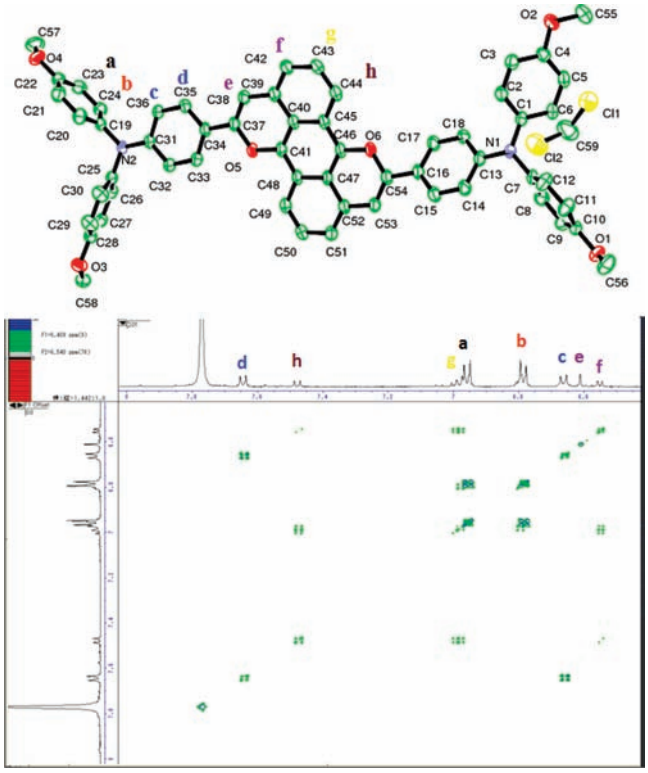

Figure 6. ORTEP diagram (50% probability, hydrogen atoms are omitted for clarity) (top) and ^{1}H 2D-COSY NMR spectra (bottom) of **[1,5-Am$_2$Pyl$_2$]^0**.

quinodimethane (Li[TCNQ]) to give a product in 51% yield that was characterized by ESI mass spectroscopy, ^{1}H and 2D-COSY NMR and XRD measurements, and elemental analysis. The ^{1}H and 2D-COSY NMR spectra of **[1,5-Am$_2$Pyl$_2$]^0** in DMF-d_7 revealed that the molecular structure of the neutral form was consistent with the pentacyclic structure, as shown in Figure 6. It should be noted that this compound was highly unstable in most solvents except DCM and dimethylformamide (DMF) under dark conditions.

Single crystals of **[1,5-Am$_2$Pyl$_2$]^0** suitable for X-ray analysis were obtained by recrystallization from DCM/hexane at 293 K under an argon atmosphere in the absence of light. An ORTEP diagram of **[1,5-Am$_2$Pyl$_2$]^0** is shown in Figure 6, and its three-dimensional packing structure is shown in Figure 7. The pentacyclic structure of the molecule was determined, and the plane of the pentacyclic moiety (C37 to C54, O5, and O6) was found to be parallel to the phenyl ring (C31−C32−C33−C34−C35−C36) of one of the triarylamine moieties. The phenyl ring (C13−C14−C15−C16−C17−C18) of the second triarylamine made a dihedral angle of 37° with the pentacyclic ring, possibly due to interactions with DCM solvent molecules (Figure 7). The high planarity of the pentacyclic ring and the adjacent two benzene rings was consistent with an expansion of the π-conjugated system upon cyclization. The C−C bond lengths in the pentacyclic moiety were in the range of 1.338(4)−1.450(4) Å, and bond lengths of C41−O5 and C46−O6 were 1.378(3) and 1.382(3) Å, respectively, suggesting an additional expansion of the π-conjugated system upon cyclization. To the best of our knowledge, this is the first example of neutral pentacyclic compounds in which the oxygen atoms are components in the flat extended π-conjugated six-membered ring.

On the basis of the structure of **[1,5-Am$_2$Pyl$_2$]^0** deduced by ^{1}H 2D-COSY NMR and single-crystal X-ray analysis, we

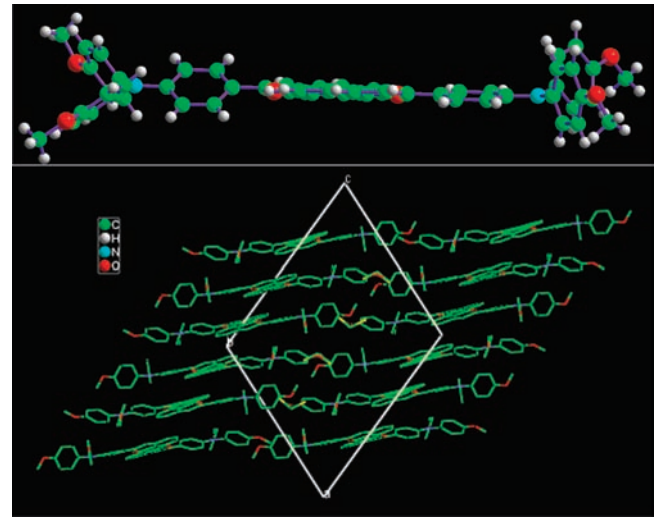

Figure 7. **[1,5-Am$_2$Pyl$_2$]^0** molecule showing planarity (top) and its three-dimensional packing structure viewed along the *b*-axis (bottom).

concluded that double protonation of the ethynyl moieties of **1,5-Am$_2$Aq** induced intramolecular cyclization by annulation of the carbonyl and ethylene groups to give a pentacyclic dipyrylium salt of **[1,5-Am$_2$Pyl$_2$]$^{2+}$** (Scheme 2).

Conclusion

We described the synthesis, characterization, chemical properties, and physical properties of the new D−A and D−A−D molecules **1-AmAq** and **1,5-Am$_2$Aq**, respectively. The former undergoes monoprotonation to give a pyrylium salt, **1-AmPyl$^+$**, which is similar in structure to **1-FcAq**. The latter undergoes a novel double proton cyclization reaction to yield the 1,5-bis(triarylamino)dipyrylium salt, **[1,5-Am$_2$Pyl$_2$](TFSI)$_2$**, with a new pentacyclic backbone by way of the monoprotonated product **[1,5-Am$_2$Pyl]TFSI**. This divalent cationic salt can be reduced to give a neutral species, **[1,5-Am$_2$Pyl$_2$]^0**, with retention of the pentacyclic backbone. The obtained condensed-ring compounds showed unique optical, electrochemical, and magnetic properties due to the very narrow HOMO−LUMO gap. In particular, the dication **[1,5-Am$_2$Pyl$_2$]$^{2+}$** showed paramagnetic behavior with two spins. These findings should be useful in designing novel functional molecular systems as well as for the synthesis via protonation reactions of novel molecules having unusual physical properties.

Experimental Section

General Method. Solvents and reagents were used as received from commercial sources unless noted otherwise. 4-Ethynyl-*N*,*N*-bis(4-methoxyphenyl)aniline was prepared by a procedure described in the literature.[18] Anhydrous solvents were obtained as guaranteed grade from Kanto Chemicals Ltd. and used after freeze−pump−thaw treatment unless noted otherwise. Triethylamine was dried by reflux over KOH, distilled under nitrogen, and degassed by freeze−pump−thaw treatment. Hexane and dichloromethane were distilled from CaH_2 under nitrogen and degassed by freeze−pump−thaw treatment. All syntheses were performed under an atmosphere of dry nitrogen or dry argon unless otherwise indicated.

NMR Measurements and Mass Spectrometry. ^{1}H and ^{13}C NMR, ^{1}H 2D-COSY NMR, ^{1}H−^{13}C HMBC, and ^{1}H−^{13}C HMQC spectra of samples in chloroform-d_1 and DMF-d_7 were collected

(18) Lambert, C.; Nöll, G.; Schmälzlin, E.; Meerholz, K.; Bräuchele, C. *Chem.—Eur. J.* **1998**, *4*, 2129–2135.

with an AL-400 (JEOL), ECX400(JEOL), or DRX500 NMR spectrometer (Bruker). ESI-TOF mass spectra were recorded with an LCT time-of-flight mass spectrometer (Micromass).

UV−Vis−Near-IR Spectroscopy in Solution. Samples for UV−vis−NIR spectroscopy in solution were prepared under an argon atmosphere. UV−vis−NIR spectra were recorded with a V-570 spectrometer (JASCO). Quartz cells with a path length of 0.1 cm were utilized to observe absorption in the UV region.

Single-Crystal X-ray Analysis. Single crystals of **1-AmAq**, **1,5-Am_2Aq**, and **[1,5-Am_2Pyl_2]^0** were mounted on a loop, and data were collected with a Rigaku AFC10 diffractometer with the Rigaku Saturn CCD system equipped with a rotating-anode X-ray generator that emits graphite-monochromated Mo Kα radiation ($\lambda = 0.7107$ Å). An empirical absorption correction using equivalent reflections and Lorentzian polarization correction was performed with the program Crystal Clear 1.3.6. The structures were solved with the program SHELXS-97[19] and refined against F^2 using SHELXL-97.[20] Pertinent crystallographic data for compounds **1-AmAq**, **1,5-Am_2Aq**, and **[1,5-Am_2Pyl_2]^0** are given in Table 1.

DFT Calculations. The geometries of **1-AmAq**, **1,5-Am_2Aq**, **[1-AmPyl]$^+$**, **[1,5-Am_2Pyl]$^+$**, **[1,5-Am_2Pyl_2]$^{2+}$**, and **[1,5-Am_2Pyl_2]^0** were fully optimized using DFT methods. The three-parameter Becke−Lee−Yang−Parr (B3LYP) hybrid exchange-correlation functional was employed. The 6-31G (p,d) basis set was used for all atoms. Based on the optimized structure, the TD-DFT method was applied to calculate the excited states relevant to the absorption spectra of each compound. The solvent effect (CH_2Cl_2) was considered using the PCM model. The present calculations were implemented using the Gaussian03 program package.[21] It should be noted that the stability of the optimized structure for **[1,5-Am_2Pyl_2]$^{2+}$** was tested using the stable=opt option to afford an unrestricted (symmetry-broken) solution. Thus, optimization of **[1,5-Am_2Pyl_2]$^{2+}$** using the unrestricted method (uB3LYP) was performed assuming either singlet or triplet states. We found that the triplet state was energetically favorable and that the energy difference between the singlet and triplet states was surprisingly small (<0.2 eV). In the triplet state, the two spins were mainly centered on the two triarylamine moieties and the pentacyclic skeleton (HOMO and LUMO shown in Figure 3). These results indicated the intrinsic character of intramolecular electron transfer in **[1,5-Am_2Pyl_2]$^{2+}$**.

Cyclic Voltammetry. A glassy carbon rod (outer diameter 3 mm, Tokai GC-20) was embedded in Pyrex glass, and a cross-section was used as a working electrode (polished with Al_2O_3 fine particles (0.3 μm diameter) and washed with purified water and acetone with ultrasonication prior to use). Cyclic voltammetry was carried out under an argon atmosphere using a platinum wire counter electrode and a Ag^+/Ag reference electrode (10 mM $AgClO_4$ and 0.1 M Bu_4NClO_4−CH_3CN solution; the $E_{1/2}$ of ferrocenium/ferrocene is 0.20 V in our conditions) using an ALS-650B voltammetric analyzer.

EPR Measurements. The spin susceptibility of the samples was measured using a JEOL FA 200 instrument. The sample solution was introduced in the sample tube and degassed by three freeze−pump−thaw cycles. Finally, the tube was sealed under a vacuum. Simulation of EPR spectra was carried out using Bruker's WIN-EPR SimFonia Software Version 1.25.

Magnetic Susceptibility Measurements. The temperature-dependent magnetic susceptibilities were measured using an MPMS superconducting quantum interference device (SQUID) spectrometer at a field length of 1 T (Quantum Design). Aluminum foil purchased from Nippaku Co. was used for the sample containers, the magnetic contributions of which were subtracted as background by measuring their individual magnetic susceptibilities at each experiment.

Synthesis of 1-AmAq. Under a N_2 atmosphere, a mixture of 1-iodoanthraquinone (2.81 g, 8.43 mmol), 4-ethynyl-*N*,*N*-bis(4-methoxyphenyl)aniline[18] (2.70 g, 8.22 mmol), bis(triphenylphosphine)palladium(II) dichloride (0.18 g, 0.41 mmol), and cuprous iodide (0.089 g, 0.47 mmol) in triethylamine (40 mL) and DMF (20 mL) was refluxed at 70 °C overnight. The color of the reaction mixture changed from yellow to dark red. After cooling to room temperature, the solvent was removed under a vacuum. The residue was dissolved in CH_2Cl_2 and washed with water, followed by drying with Na_2SO_4. The product was purified on an Al_2O_3 (II−III) column and eluted with a 1:2 ratio of CH_2Cl_2/hexane to give a 10% yield. Anal. Calcd for $C_{36}H_{25}NO_4$: C, 80.73; H, 4.70; N, 2.62. Found: C, 80.56; H, 4.85; N, 2.42. ^{1}H NMR ($CDCl_3$, 400 MHz): δ 3.82 (s, 6H), 6.86 (d, 4H, $J = 8.8$ Hz), 6.90 (d, 2H, $J = 8.8$ Hz), 7.10 (d, 4H, $J = 8.8$ Hz), 7.51 (d, 2H, $J = 8.8$ Hz), 7.71 (t, 1H, $J = 7.8$ Hz), 7.79 (m, 2H), 7.94 (m, 1H), 8.28 (d, 2H, $J = 7.8$ Hz), 8.35 (m, 1H).

Synthesis of 1,5-Am_2Aq. Under a N_2 atmosphere, a mixture of 1,5-dibromoanthraquinone (0.607 g, 1.66 mmol), 4-ethynyl-*N*,*N*-bis(4-methoxyphenyl)aniline[18] (1.152 g, 3.50 mmol), bis(triphenylphosphine)palladium(II) dichloride (0.233 g, 0.33 mmol), and cuprous iodide (0.127 g, 0.66 mmol) in triethylamine (100 mL) was refluxed at 70 °C for 3 h. The color of the reaction mixture changed from yellow to dark red. After cooling to room temperature, the solvent was removed under a vacuum. The residue was dissolved in CH_2Cl_2 and washed with water, followed by drying with Na_2SO_4. The product was purified on an Al_2O_3 (II−III) column and eluted with a 1:1 ratio of CH_2Cl_2/hexane to give a 38% yield. Anal. Calcd for $C_{58}H_{42}N_2O_6 \cdot 1.3H_2O$: C, 78.59; H, 5.07; N, 3.16. Found: C, 78.67; H, 5.08; N, 2.86. MS (ESI-TOF): $m/z = 862.56$ (calcd M^+ 862.30). ^{1}H NMR ($CDCl_3$ 400 MHz): δ 3.83 (s, 12H), 6.86 (d, 8H, $J = 9.0$ Hz), 6.90 (d, 4H, $J = 9.0$ Hz), 7.08 (d, 8H, $J = 9.0$ Hz), 7.51 (d, 4H, $J = 9.0$ Hz), 7.70 (t, 2H, $J = 7.8$ Hz), 7.91 (dd, 2H, $J = 7.7$ Hz, 1.5 Hz), 8.31 (dd, 2H, $J = 7.7$ Hz, 1.5 Hz).

Synthesis of [1-AmPyl]TFSI. Under an argon atmosphere, **1-AmAq** (0.040 g, 0.14 mmol) was dissolved in 10 mL of CH_2Cl_2 and stirred. To this was added bis(trifluoromethanesulfone)imide (0.105 g, 0.373 mmol) in 3 mL of CH_2Cl_2. After stirring for 60 min, the color of the solution changed gradually from red to green, after which 60 mL of hexane was added. The mixture was allowed to crystallize overnight. The dark precipitate was filtered off using a membrane filter and washed with hexane. **[1-AmPyl]TFSI** was obtained in 32% yield. Anal. Calcd for $C_{38}H_{26}N_2O_8S_2F_6$: C, 55.88; H, 3.21; N, 3.43. Found: C, 55.73; H, 3.43; N, 3.23. ^{1}H NMR (CD_2Cl_2, 400 MHz): δ 3.86 (s, 6H), 6.95 (d, 4H, $J = 9.0$ Hz), 7.01 (d, 2H, $J = 9.0$ Hz), 7.20 (m, 4H), 8.00 (m, 2H), 8.05 (m, 2H), 8.20 (m, 1H), 8.45 (m, 1H), 8.51 (m, 1H), 8.54 (m, 1H), 8.58 (m, 1H), 8.65 (s, 1H).

Synthesis of [1,5-Am_2Pyl]TFSI and [1,5-Am_2Pyl_2](TFSI)$_2$. Under an argon atmosphere, **1,5-Am_2Aq** (0.100 g, 0.12 mmol) was dissolved in 10 mL of CH_2Cl_2 and stirred. To this was added bis(trifluoromethanesulfone)imide (0.033 g, 1.19 mmol for **[1,5-Am_2Pyl]TFSI** and 0.130 g, 4.63 mmol for **[1,5-Am_2Pyl_2](TFSI)$_2$**) in 3 mL of CH_2Cl_2. The color of both solutions changed from red to dark green. After stirring for 30 min, 20 mL of hexane was added. The mixtures were allowed to crystallize overnight. The dark precipitates were filtered off using a membrane filter and washed with hexane. **[1,5-Am_2Pyl_2]TFSI** and **[1,5-Am_2Pyl_2](TFSI)$_2$** were obtained in 89% and 92% yields, respectively. Anal. Calcd for $C_{60}H_{43}N_3F_6O_{10}S_2 \cdot 0.5CH_2Cl_2$: C, 59.46; H, 3.63; N, 3.44. Found: C, 59.71; H, 3.72; N, 3.52. Anal. Calcd for $C_{62}H_{44}N_4F_{12}O_{14}S_4$: C, 52.25; H, 3.11; N, 3.95. Found: C, 52.31; H, 3.46; N, 3.98. MS (ESI-TOF): $m/z = 864.00$ (calcd M^+ 864.32).

Synthesis of [1,5-Am_2Pyl_2]^0. Under a N_2 atmosphere, **[1,5-Am_2Pyl_2](TFSI)$_2$** (0.020 g, 0.014 mmol) was dissolved in a solvent mixture composed of CH_2Cl_2 (10 mL) and CH_3CN (10 mL) and stirred without exposure to light. To this reaction mixture was added Li[TCNQ] (0.006 g, 0.028 mmol). The color of the solution changed from dark green to red. After stirring for 2 h, the solvent was

(19) Sheldrick, G. M. *Program for Crystal Structure Solution*; University of Göttingen: Germany, 1997.
(20) Sheldrick, G. M. *Program for Crystal Structure Refinement*; University of Göttingen: Germany, 1997.
(21) Frisch, M. J.; et al. *Gaussian 03*, revision-B.05; Gaussian, Inc.: Pittsburgh, PA, 2003.

removed under a vacuum. The dark reddish product was purified on an Al_2O_3 (II−III) column and eluted with CH_2Cl_2. The pink fraction was collected, and the solvent was removed by evaporation. The red product was further purified on a silica gel column and eluted with a 5:1 ratio of CH_2Cl_2/hexane. The first pink fraction was collected and recrystallized in CH_2Cl_2/hexane. This compound was sensitive to light; purification was performed without exposure to light. **[1,5-Am$_2$Pyl$_2$]^0** was obtained in 51% yield. Anal. Calcd for $C_{58}H_{44}N_2O_6 \cdot 0.5CH_2Cl_2$: C, 77.43; H, 5.00; N, 3.09. Found: C, 77.60; H, 5.08; N, 2.93. MS (ESI-TOF): $m/z = 864.306$ (calcd M^+ 864.319). ^{1}H NMR (DMF, 400 MHz): δ 3.60 (s, 12H), 6.55 (d, 2H, $J = 6.6$ Hz), 6.61 (s, 2H), 6.66 (d, 4H, $J = 9.0$ Hz), 6.79 (d, 8H, $J = 9.0$ Hz), 6.94 (d, 8H, $J = 9.0$ Hz), 6.99 (t, 2H, $J = 6.8$ Hz), 7.49 (d, 2H, $J = 9.0$ Hz), 7.64 (d, 4H, $J = 9.0$ Hz).

Acknowledgment. This work was supported by Grants-in-Aid from MEXT of Japan (Nos. 20245013 and 21108002, area 2107 (Coordination Programming)) and the Global COE Program for Chemistry Innovation. The authors acknowledge Rigaku Corporation for single-crystal X-ray data of **[1,5-Am$_2$Pyl$_2$](TFSI)$_2$**.

Supporting Information Available: X-ray crystallographic information files (CIF) for **1-AmAq**, **1,5-Am$_2$Aq**, and **[1,5-Am$_2$Pyl$_2$]^0**; synthetic schemes, details of single-crystal X-ray analysis, tables of excitation energies, spectra, voltammograms, and an ORTEP diagram of **[1,5-Am$_2$Pyl$_2$](TFSI)$_2$**; complete refs 8b and 21. This material is available free of charge via the Internet at http://pubs.acs.org.

JA105250F